Drying Technology

An International Journal

ISSN: (Print) (Online) Journal homepage: https://www.tandfonline.com/loi/ldrt20

Airborne power ultrasound for paper drying: an experimental study

Zahra Noori O'Connor & Jamal S. Yagoobi

To cite this article: Zahra Noori O'Connor & Jamal S. Yagoobi (2023): Airborne power ultrasound for paper drying: an experimental study, Drying Technology, DOI: 10.1080/07373937.2023.2188415

To link to this article: https://doi.org/10.1080/07373937.2023.2188415

DRYING TECHNOLOGY
https://doi.org/10.1080/07373937.2023.2188415

Taylor & Francis
Taylor & Francis Group

Airborne power ultrasound for paper drying: an experimental study

Zahra Noori O'Connor[a,b] and Jamal S. Yagoobi[a,b]

[a]Center for Advanced Research in Drying, Worcester Polytechnic Institute, Worcester, MA, USA; [b]Multi-Scale Heat Transfer Laboratory, Mechanical and Materials Engineering Department, Worcester Polytechnic Institute, Worcester, MA, USA

ABSTRACT

A novel approach for paper drying using airborne ultrasound technology is presented. A unique experimental setup is developed, and a systematic study is conducted using 2^3 factorial design of experiments and Analysis of Variance. Three controlling factors are considered in the experiments including the initial moisture content, basis weight and refining condition. The outcome of the experiments is compared to a previous work on direct-contact ultrasonic drying of paper. The results confirm that similar to direct-contact, for airborne ultrasonic drying, the basis weight/thickness of the sample is the most important factor in ultrasonic drying and it is followed by the effect of initial moisture content. Using linear regression model, a correlation for predicting the total time of ultrasonic drying is provided. Quality of the dried samples is evaluated, and the permeability measurements confirmed the effect of pore characteristics on ultrasonic drying. The analysis for energy consumption reveals that airborne ultrasonic drying is more efficient at higher moisture contents.

ARTICLE HISTORY
Received 12 December 2022
Revised 2 March 2023
Accepted 4 March 2023

KEYWORDS
Airborne ultrasonic drying; non-contact ultrasonic drying; paper drying; energy analysis

1. Introduction

Drying, defined as water removal from a moist medium, is one of the most energy intensive processes in industrial applications and it plays an important role in global economy. Drying is an essential operation in industries such as pulp and paper, chemical, food, agricultural, polymer, ceramics, wood, and mineral processing. The current drying technologies are mostly dependent on conduction and convection thermal heating. As reported by the US Department of Energy,[1] 5.27×10^{17} J/year of total energy in drying processes (1.27×10^{18} J/year) can be saved by applying non-thermal drying technologies. Therefore, it is crucial to develop sustainable and efficient drying technologies to decrease the industrial energy consumption and carbon footprint. In the last few decades, specific attention has been paid to progression of hybrid drying technologies such as ultrasonic drying,[2] microwave drying,[3] electrohydrodynamic drying,[4,5] infrared drying,[6] plasma drying,[7] and pulsed vacuum drying,[8] mostly in combination with heating.

Drying using ultrasound mechanism is not a new idea and to the best of the authors' knowledge, Burger and Sollner[9] were the first to consider removal of water from wet quartz sands using ultrasonic drying, in 1936. Since then, many studies have been devoted to the application of ultrasonic drying in direct-contact, and airborne (non-contact) mechanisms. Direct-contact ultrasonic drying requires the material to be in direct contact with the vibrating structure and it uses high-frequency ultrasound waves which can be higher than 1 MHz. According to Gallego-Juarez et al.,[10] direct-contact ultrasound efficiently enhances the sound energy transfer from the transducer to the materials. This technology most recently was used for fabric drying.[11] For non-contact or airborne ultrasonic drying, the ultrasonic waves travel to the material through air, and it uses high-power waves that are in the range of 20–100 kHz. Fairbanks[12] compared two cases of drying of wet coal particles: (1) in direct contact with the vibrating surface and (2) using non-contact ultrasound. It appeared that the effectiveness of ultrasonic drying was much higher in the direct-contact ultrasonic drying. Another observed difference between these two drying cases was that the effect of heating in direct-contact ultrasonic drying is much higher than non-contact ultrasonic drying. Tao et al.[13] compared airborne ultrasonic drying and contact ultrasonic drying to intensify air drying of blackberries and they reported that in presence of ultrasound, the drying process was accelerated, the

CONTACT Zahra Noori O'Connor znoori@wpi.edu 100 Institute Rd, Mechanical Engineering Department, Worcester, MA 01609, USA.

energy consumption was reduced, and retention of organic acids in blackberries was enhanced. Zhang and Abatzoglou[14] stated two challenges related to direct-contact ultrasonic drying: First, the heating effect may not be desirable in terms of the quality of the dried products. Second, since the product must be in direct contact with the transducer, this technology is not easily adaptable to the current convective dryers. Hence, in this regard, non-contact ultrasonic drying is the most ideal in terms of adaptation to the conveyer dryers. Non-contact ultrasonic drying has been widely used in food conservation industries,[15–17] especially in the current century. However, to the best of the authors' knowledge, ultrasonic drying has not been used for paper drying. Recently Noori O'Connor et al.[18] employed direct-contact ultrasonic drying for drying of hand-sheet papers for both hardwood and softwood pulps. Using design of experiments and Analysis of variance, they concluded that sample basis weight/thickness and initial moisture content have the maximum effect on the total time of ultrasonic drying. Their results also revealed that at higher moisture contents, ultrasonic atomization becomes more effective. In the current study, for the first time, a unique experimental setup for airborne ultrasonic drying will be employed for paper drying. Using ANOVA analysis, the impact of different parameters corresponding to the typical entry conditions in papermaking machines will be investigated. The outcome of this research will be compared with direct-contact ultrasonic drying of paper in terms of heating effects, drying rate, final product quality, and energy efficiency. Therefore, a complete package of the potentials of ultrasonic drying for paper drying will be provided.

2. Experimental setup and methods

2.1. Experimental setup

A unique experimental setup was designed and assembled as shown in Figure 1. The main components include the transducer part, electric power generator or EPG (power amplifier and dynamic resonance controller) and sample holder. The sample holder is a stainless steel mesh with 5 mm size circular holes to allow for the moisture mist to escape from the underneath of sample as well. The sound level around the transducer in free field is about 160 dB. For safety purposes, composite double layers soundproofing foams (quiet barrier specialty composite, Soundproofing Cow company, Pennsylvania, USA) were used to reduce the sound level around the transducer to less than 80 dB. It should be noted that this is an open system, and the door of the setup was kept open during the experiments. This airborne transducer and EPG was purchased from Pusonics S.L. (Madrid, Spain). According to the manufacturer,[19] the transducer is composed of a piezoelectric Langevin-type sandwich, a mechanical amplifier or horn, and an extensive radiator, that provides the required impedance to match with the media. The transducer plate is made from titanium and its dimensions are 43.3×23.4×3.14 cm. In this study, the ultrasound power is 225 W (the maximum power recommended by the manufacturer) and working frequency is 21 kHz. The weight of the samples was measured intermittently at 2 min intervals using a microbalance (Sartorius BCE6200, Gottingen, Germany, with 0.001 g accuracy). The samples' thickness was gauged using a digital thickness gauge with 0.002 mm accuracy.

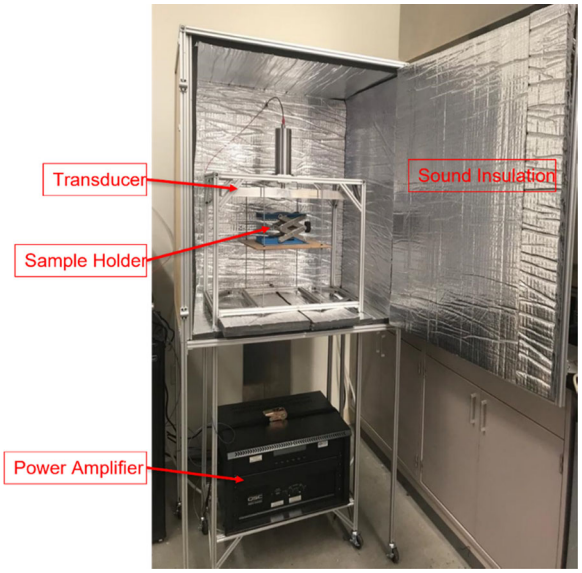

Figure 1. The experimental setup for non-contact ultrasonic drying.

The pulps used in this study, refined and unrefined softwood, were Northern Bleached Softwood Kraft (NBSK). The refining is performed using an industrial Disk refiner with energy about 3-5 horsepower day/-tone (hpdt). The Canadian Standard Freeness (CSF) value for the unrefined pulp is 757 ml and for the refined pulp is 300 ml. The hand-sheet making procedure was followed according to TAPPI T205 standard to reach to 150% and 200% dry-basis moisture contents (DBMC). The refined pulp was a slurry with 4% consistency and by adding water, the targeted initial weight was obtained. The unrefined pulp was a dried sheet that was disintegrated in water to reach to the desired consistency. The pulp consistency is

defined as the percentage by weight of oven-dry fibers in a stock suspension (slurry). The initial diameter of the hand-sheets was 15.9 cm.

The uncertainty analyses for the derived quantities are represented in Table 1 and were done according to the method discussed by Kline and McClintock.[20] For these calculations, the number of trial points is three.

The results of ultrasonic drying are compared to conductive thermal drying experiments using a hot plate (Corning PC-420D). In this case, the samples were simply placed on top of hot plate maintained at 40 °C.

For colorimeter measurements, ColorFlex EZ, HunterLab (Virginia, USA) was used based on CIELAB color space ($\boldsymbol{L}^*\boldsymbol{a}^*\boldsymbol{b}^*$). For paper drying, Brightness Index (BI) is an important criterion depending on the application of the paper and it can be calculated using the following equation:

$$BI = 100 - \sqrt{(100 - L^*)^2 + (a^{*2} + b^{*2})} \qquad (1)$$

where $\boldsymbol{L}^*$ is the lightness index, $\boldsymbol{a}^*$ is red-greenness index and $\boldsymbol{b}^*$ is yellow-blueness index. For the tensile strength measurements, Multitest-dV motorized force tester from Mecmesin (West Sussex, UK) device was employed using rectangular samples. To be able to compare the tensile strength results with those of direct-contact ultrasonic drying, identical samples were used (19.8 mm in length and 5 mm in width). The distance between the grips was fixed at 9 mm.

In addition, Model 4340 Automatic Densometer & Smoothness Tester from Gurley (New York, USA) was used to measure Gurley seconds for each sample, following the procedure of Gurley methods (TAPPI standard T460). The Gurley second or Gurley unit is a unit that describes air permeability as a function of the time required for a specified amount of air to pass through a specified area of a separator under a specified pressure. Darcy's law then was used to calculate the permeability of the paper samples:

$$Q = \frac{kA}{\mu L}\Delta P \qquad (2)$$

where Q is the volumetric air flow (m^3/s), k is permeability (m^2), A is the opening area (m^2), μ is dynamic viscosity of fluid (kg/m.s), L is the sample thickness (m), and ΔP is the pressure drop across the sample (Pa). The value of Q is 100 cc and A is 6.45 cm^2 (for a circular area of paper) using a pressure differential of 1.22 kPa.

Table 1. The derived uncertainty of experimental data.

Derived Quantity	Maximum Uncertainty
DBMC	± 6.2%
Brightness index	± 0.5%
Permeability	± 5.7%
Energy factor	± 4.24%

The temperature measurements are conducted using fiber optic sensors (Micronor, TS3, California, USA) and a signal conditioner (Micronor, FOTEMP4-PLUS, California, USA).

All experiments are conducted at room conditions (20 °C and 50% humidity).

2.2. Experimental method

The method applied for analyzing the experimental results was 2^3 factorial design of experiments (DOE). This method allows to understand the individualized effect of the controlling factors as well as their interactive effects. The three main factors in this research include the initial DBMC, basis weight and refining condition. Table 2 indicates the high and low levels for these three factors. Each sample is repeated three times and the points in Table 2 are randomized in order. The measured final thickness for each sample is provided for comparison purposes. The typical moisture content at the entry of dryer section in paper drying is 100-150% DBMC. Higher moisture content (200% DBMC) allows to consider the application of ultrasound drying in upstream of the dryer section. The range of the parameters is chosen based on consulting with the related industry. For simplicity, the abbreviations provided in Table 2 are employed in this paper. The last row of the table is the center point of the cube. The center point is halfway between the low and high levels and its importance comes to play when replicating the cube is expensive and time consuming. The centerpoints are repeated five times in a randomized order. Analysis of Variance (ANOVA) was applied for the statistical analysis using Minitab software and p-values less than 0.05 were considered statistically significant. Linear regression analysis was done to investigate the effect of the controlling factors on the total time of ultrasonic drying.

The data for direct-contact ultrasonic drying of paper samples are used from Noori O'Connor et al.[18]

3. Results and discussion

3.1. Thermal effect of airborne ultrasonic drying

An infrared image of the transducer plate from the side view is shown in Figure 2. The maximum temperature at the bottom of the plate is 40 °C. The right

Table 2. High and low levels of factors for 2^3 factorial design of experiments for softwood (S) fibers. R defines refined and unR defines unrefined.

	Factors			
Abbreviations	Initial DBMC (%)	Basis Weight (g/m^2)	Refining Condition	Final Thickness (mm)
S-unR-150-160	150	160	Unrefined	0.32
S-unR-200-160	200	160	Unrefined	0.32
S-unR-150-325	150	325	Unrefined	0.67
S-unR-200-325	200	325	Unrefined	0.67
S-R-150-160	150	160	Refined	0.2
S-R-200-160	200	160	Refined	0.2
S-R-150-325	150	325	Refined	0.47
S-R-200-325	200	325	Refined	0.47
S-Center Point	175	242	50% R & 50% unR	0.57

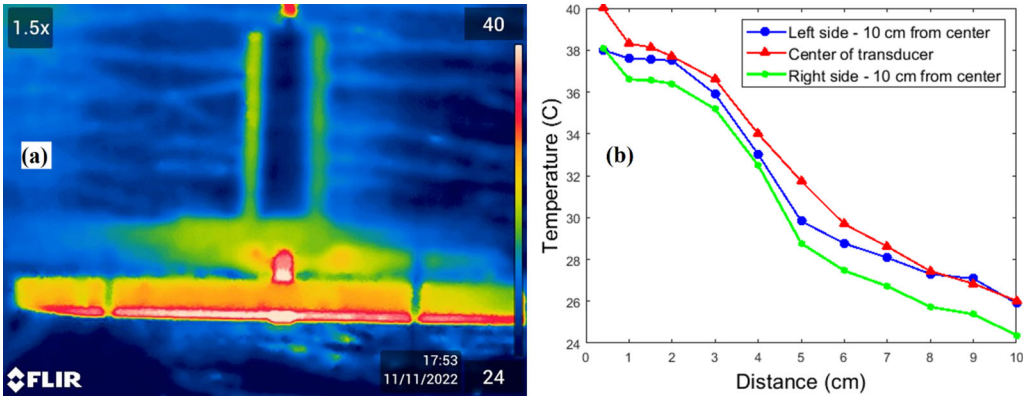

Figure 2. Infrared image of the side view of the transducer plate (a) and the effect of distance from the plate on temperature (b).

hand side plot shows the measured temperatures at different distances underneath the transcuer plate at three different locatins. Figure 2 shows that at a fixed distance from the plate, the temperature difference between the center and the two sides of the rectangular plate is about 2 °C and the temperature decreases as the distance increases. In addition to the conversion of electrical power to heating energy in the plate, part of the temperature rise underneath the transducer plate is due to the absorption of ultrasonic waves. These observations agree with literature such as.[15,21–23] Therefore, unlike the direct-contact ultrasonic drying, which the transducer's temperature increased up to 80 °C during drying,[18] non-contact ultrasonic drying has less impact on the moist sample temperature compared to direct-contact ultrasonic drying. Hence, as stated by Zhang and Abatzoglou,[14] the heating effect can be much more important in direct-contact ultrasonic drying and depending on the application, it may be beneficial or disadvantage for the process.

To measure the temperature inside the sample underneath the transducer, a sandwich of two identical handsheets are made and three fiber optic thermocouples are mounted in between them at 3 mm distance from the sample's surface. One thermocouple is placed in the center of the sample and the other two thermocouples are fixed at 7 cm distance to the right and left of the center. The two handsheets are refined softwood with initial moisture contents of 150%. The weight of each sample is chosen such that the total basis weight of the sandwich is 325 g/m^2 (about 0.6 mm thickness). One thermocouple is placed at the center and two other thermocouples are placed 7 cm away from the center in the diameter of the handsheet. The sandwich sample is placed underneath the transducer in the longitudinal direction. Figure 3 shows the results of temperature measurements inside the sandwich. There are some fluctuations in the temperature in time and one reason could be the movement of air (compression and contraction cycles) by the ultrasonic waves underneath the transducer or change in the conditions of the sample during drying. The temperature at the center of the sample has the maximum value compared to the other two temperatures. The trend is that initially the thermocouples are at room temperature but when it is placed underneath the transducer, the temperature increases. As the sample gets dried, the amount of energy consumed for evaporation decreases and as a result, the temperature increases by time. At the end, when the sample is

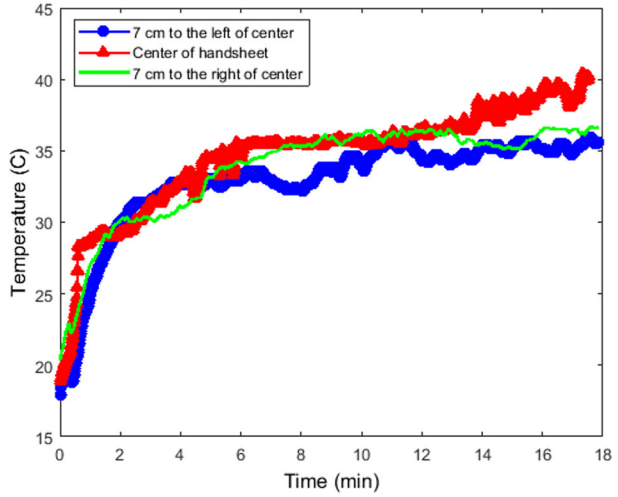

Figure 3. Temperature measurements inside a sandwich sample during airborne ultrasonic drying for S-R-150-325.

completely dried, the temperature reaches to the maximum temperature measured in free field from Figure 2 above.

The decrease in the temperature by increasing the distance from the plate is due to the fact that the average sound pressure level at planes parallel to the plate decreases by increasing the distance. From the information provided by Pusonics S.L., the maximum sound energy is at 4 mm distance from the plate. To confirm this observation, the drying curves of a similar sample at different distances from the transducer plate are illustrated in Figure 4. It is obvious that the drying curve slope is maximum at 4 mm distance from the plate and the drying time increases by increasing the distance. Therefore, in the following experiments, the distance between the transducer plate and the sample is fixed at 4 mm in all experiments.

3.2. Comparing airborne ultrasonic drying with conductive heat drying

Since the temperature rises up to 40 °C at 4 mm underneath the transducer, the airborne ultrasonic drying is compared with conductive drying at 40 °C in Figure 5. In the hot plate drying, the sample is under no tension and in this case the sample is directly placed on top of the hot plate. For conductive heat drying, the sample must be in direct contact with the hot plate to have the maximum efficiency and therefore, no mesh sample holder is used. However, for the case of airborne ultrasonic drying, a mesh sample holder is used to increase the efficiency of drying as it allows the drying to occur from the bottom of the sample as well as the top. It is illustrated in Figure 5 that the airborne ultrasonic drying decreases the drying time by 9% compared to the hot plate drying. It should be noted that part of this increase in drying rate for airborne ultrasonic drying compared to conductive heat drying is related to employing a mesh sample holder in ultrasonic drying. The favorable impact of airborne ultrasonic drying on quality of the dried sample will be discussed in the next sections.

3.3. Analysis of the factorial design of experiments

The drying curves for the ultrasonically dried samples are shown in Figure 6. The final DBMC of the dried samples is ∼3%. As an example, the drying experiment at the center point was repeated four times. Each drying curve can be split into a constant drying rate region followed by a falling drying rate region. The constant drying rate corresponds to free water removal and the falling drying rate is governed by the

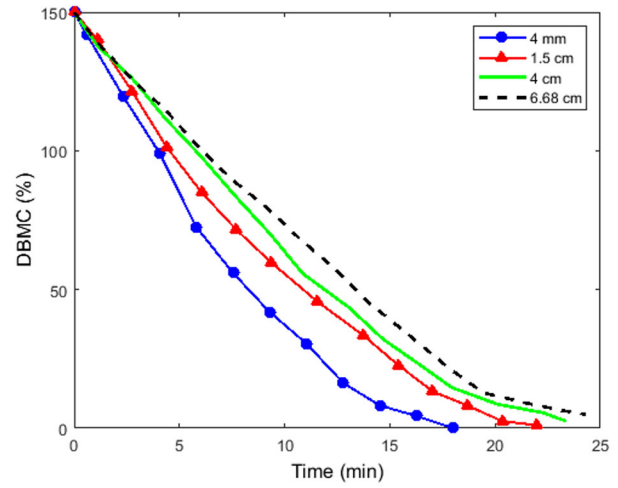

Figure 4. The effect of distance from the plate on drying curves for S-R-150-160 sample.

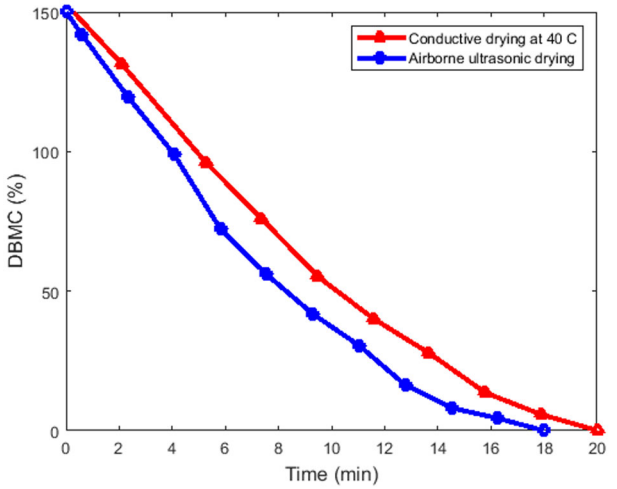

Figure 5. Comparing the drying curves for airborne ultrasonic drying and conductive heating at 40 °C for S-R-150-160.

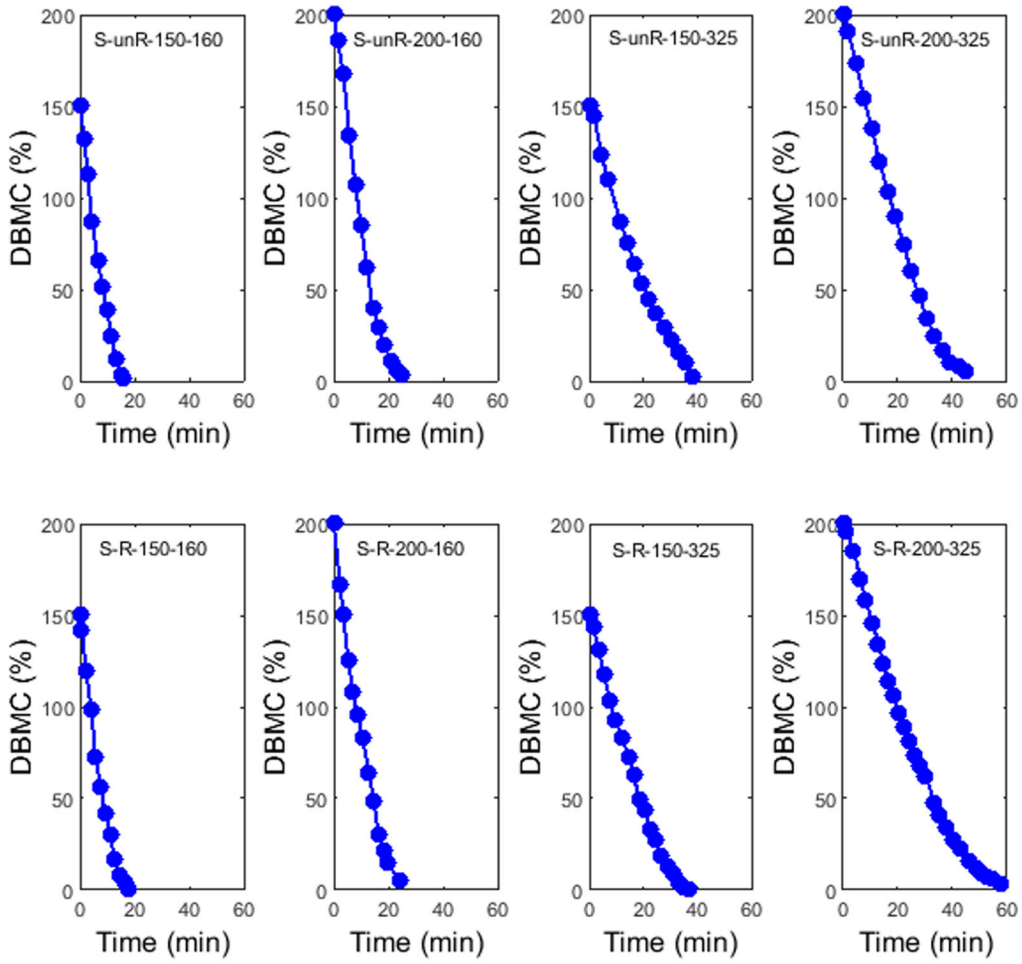

Figure 6. Drying curves for airborne ultrasonic drying of paper samples.

removal of the associated water (also known as bound water). The same behavior was observed for the direct-contact ultrasonic drying[18] and this is typical regardless of the drying mechanism.

In Figure 6, increasing the initial moisture content, slightly increases the drying time, especially at higher basis weights, since the thickness of the sample is higher, the water removal is slower. In general, unrefined samples dry faster than refined samples and it is predicted due to the difference in pore structure and fiber characteristics. The unrefined fibers are longer in length and larger in diameter compared to refined fibers and it results in higher pore volume and thickness in unrefined samples. Therefore, the shortest and longest drying times correspond to S-unR-150-160 and S-R-200-325, respectively. In general, the pores allow the ultrasonic waves to easily reach the inner structure of the paper being dried; hence, higher open pore porosity makes the ultrasonic drying to be more efficient. More details on the effect of pore characteristics and permeability measurements will be discussed in section 3-5-3.

In order to analyze the results more systematically, 2^3 factorial design of experiments are used for the total time of ultrasonic drying.

3.4. Importance of the controlling factors on total time of ultrasonic drying

The results of Analysis of Variance (ANOVA) for the total time of ultrasonic drying are summarized in the pareto chart of the standardized effects represented in Figure 7. The pareto chart allows to detect the factor and the interactive effects that are most influential. The absolute values are shown from the largest effect to the smallest effect. According to Figure 7, in the range of the studied parameters, basis weight has the maximum effect on the total time of ultrasonic drying followed by the initial moisture content. The interactive effects of the factors are less important in this analysis. This agrees with the results of direct-contact ultrasonic drying from Noori O'Connor et al.[18] The outcome of linear regression analysis for the total time of drying is reported in Table 3. The coefficient

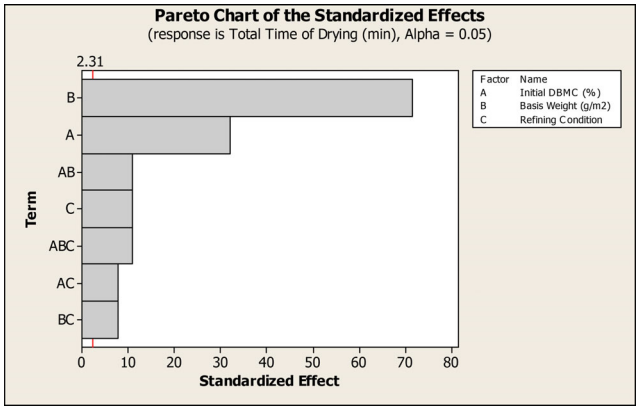

Figure 7. Pareto chart of the standardized effects for total time of ultrasonic drying.

of determination for this analysis is 99.8%, and zero p-values implies that the predicted correlation by linear regression analysis is adequate for describing the total time of ultrasonic drying. Since the refining condition is a qualitative data, the numeric values of −1 and 1 are considered for unrefined and refined, respectively. The relationship between the total time of ultrasonic drying and the factors is described as:

$$Total\ Drying\ Time = \beta_0 + \sum_{i=1}^{k} \beta_i X_i + \sum_{i=1}^{k} \sum_{j=1}^{k} \beta_{ij} X_i X_j + \beta_{123} X_1 X_2 X_3 \quad (3)$$

where k is the number of factors, and X_i (i = 1, 2, 3) are the controlling factors. β_0 is the constant coefficient, β_{ij} are the coefficients for the interactive effects of factors and β_{123} captures the interactive effect of all the three factors. Factors 1, 2, and 3 are defined as initial DBMC, basis weight, and refining condition, respectively.

3.5. Quality measurements

The quality of the ultrasonically dried samples such as the color and tensile strength plays a significant role in terms of application of the paper. This section is devoted to the quality measurements of the handsheet papers dried by non-contact ultrasound mechanism. In addition, in support of the above discussions to relate the pore characteristics and the drying behavior, permeabilities of the samples are measured.

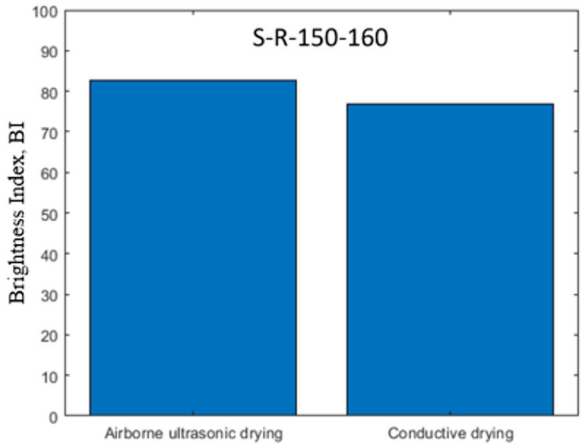

Figure 8. Comparing the brightness indices of an ultrasonically dried sample with a sample dried using conductive heating at 40 °C. The maximum standard deviation is 0.04.

3.5.1. Colorimeter measurements

To compare the impact of drying method, brightness indices of a sample dried using airborne ultrasonic drying and a similar sample dried by conductive drying are compared in Figure 8. It is shown that direct heating in conductive drying reduces the brightness index of the sample compared to airborne ultrasonic drying. This is due to the thermal effect at a longer time when the sample is in direct contact with the hot plate. The reported data for colorimeter measurements are an average of three measurements from each side of the handsheet.

Figure 9 shows the brightness indices of different samples dried using airborne ultrasonic drying. The unrefined samples have higher brightness index, and by increasing the initial moisture content and basis weight, the brightness index increases slightly. These observations are due to increasing the porosity of the sample by increasing the initial moisture content and the basis weight according to the measurements in.[18] In fact, lightness is a subjective measure of perceived light and higher porosity leads to higher lightness and therefore higher brightness index. The results generally agree with the results for the direct-contact ultrasonic drying published by Noori O'Connor et al.[18] In that paper, the authors compared the brightness index of an ultrasonically dried sample with a sample dried using conductive heating at 80 °C and observed that direct-contact ultrasonic drying slightly improves the brightness index.

The results of linear regression for brightness index are reported in Table 3. For these samples, basis

Table 3. Coefficients for equation (1) calculated from linear regression analysis.

		β_0	β_1	β_2	β_3	β_{12}	β_{13}	β_{23}	β_{123}	R^2 (%)
Softwood	Drying time (min)	−6.47	0.024	0.006	31.68	0.0008	−0.194	−0.163	0.001	99.8
	Brightness index	79.32	0.0126	0.0088	6.08	6.27×10^{-6}	−0.03	−0.026	9.97×10^{-5}	99.7

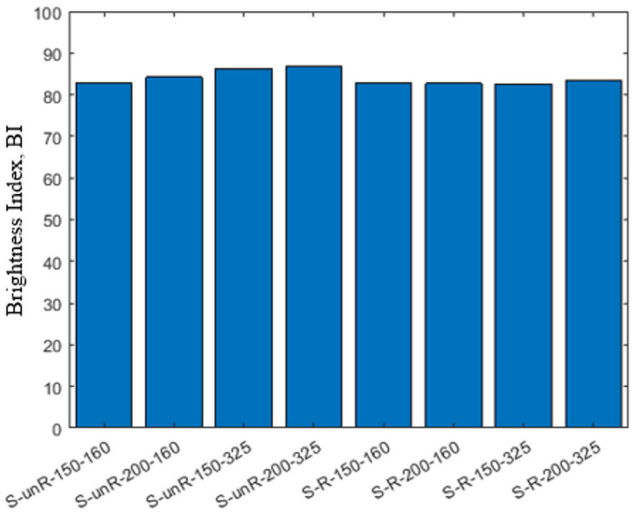

Figure 9. Brightness indices of ultrasonically dried paper samples. The maximum standard deviation is 0.02.

weight followed by the initial DBMC has the highest effects on the brightness index.

3.5.2. Tensile strength measurements

Figure 10 compares the tensile strength of a sample dried using airborne ultrasonic drying with a sample thermally dried at 40 °C in contact with a hot plate. The tensile strain is almost the same for the two samples, but the sample dried using ultrasonic drying has a slightly higher tensile stress, which is favorable for the end product. This could be explained by the difference in the mechanism of airborne ultrasonic drying versus contact heat drying and the impact of that on the shrinkage of paper, total strain during drying, and pore structure. It is suggested to measure these characteristics in the future investigations of ultrasonic drying of paper. Mäkelä[24] reported that the tensile strength of paper is dependent on the total strain during drying and it is independent of the drying temperature, final drying time, and drying constraint history. In general, less shrinkage during drying creates higher paper strength.

Figure 11(a) and (b) compare the tensile strength measurements for refined and unrefined softwood samples, respectively. The initial moisture content does not have significant impact on the tensile strength measurements and hence, only the tensile strength for the samples with 150% DBMC are provided. The refined samples have higher ultimate tensile stress (UTS) compared to that of unrefined samples. This is due to the fact that refining of the pulp results in increase of sheet density and thus, better tensile strength. Similar to the direct-contact ultrasonically dried samples, due to the effect of the grips, the sample with higher basis weight and thickness has a lower UTS. It should be mentioned that the tensile strength of the samples dried using direct-contact from[18] and non-contact ultrasonic drying completely agree, qualitatively. The slight quantitate difference may come from the difference in the thickness and the source of the pulps. Table 2 provides the thickness of the dried samples using airborne ultrasonic drying and the thickness of the samples dried by direct-contact ultrasonic drying can be found in.[18] Table 4 summarizes the mechanical strengths of the samples.

3.5.3. Permeability measurements

One of the pore characteristics of the paper that has a significant impact on its drying behavior is permeability. Permeability is a paper property that allows gasses

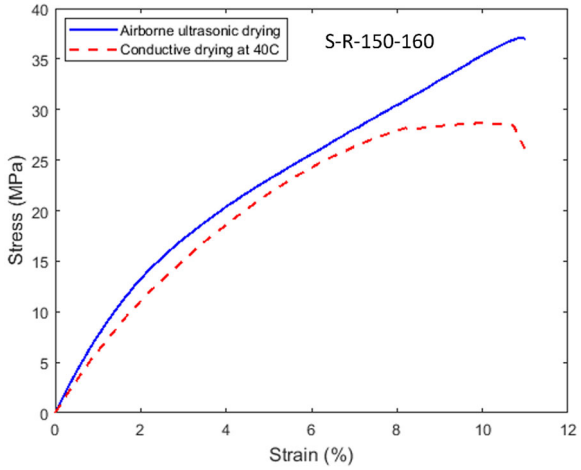

Figure 10. Comparing stress-strain curves for an ultrasonically dried sample with a sample thermally dried at 40 °C in contact with a hot plate. The maximum standard deviation is 2.4.

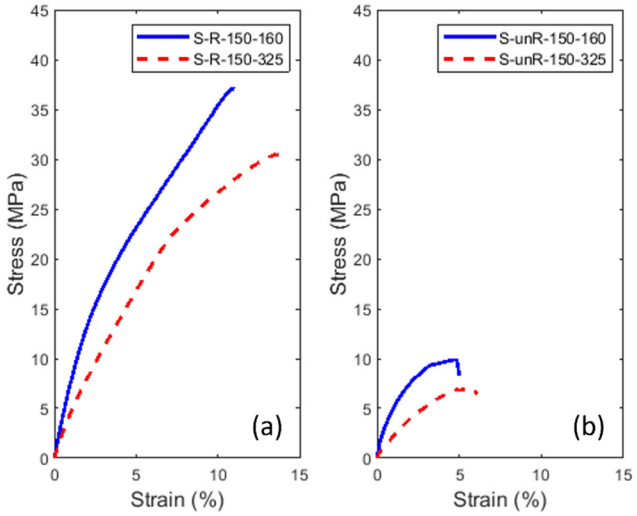

Figure 11. Stress-strain curves for (a) refined softwood samples and (b) unrefined softwood samples. The maximum standard deviation is 3.1.

Table 4. Ultimate tensile strain and ultimate tensile stress for different softwood samples.

Sample	Ultimate Tensile Strain (%)	Ultimate Tensile Stress (MPa)
S-unR-150-160	5.01	9.86
S-unR-150-325	6.06	6.92
S-R-150-160	11	37.13
S-R-150-325	14	30.43
S-R-150-160 (Conductive drying)	10.73	28.64

(air) or liquids to pass through it under a pressure difference across a sheet. Permeability is determined by measuring the rate of airflow through a known area of the paper sheet. Table 5 shows the mean values and standard deviations of the Gurley seconds for 5 measurements and the calculated permeability.

The permeability of the unrefined samples is 10 times higher than refined samples. This comes from the fact that refining of the pulp leads to a better sheet formation and the refined handsheet is more compact, as can be concluded by comparing the thicknesses for refined and unrefined samples in Table 2. Permeability is determined by the fraction of open pores and the size of the pores and in general, higher porosity results in higher permeability. The permeability decreases by increasing the basis weight. These measurements agree with Figure 6, which S-R-150 or 200%-325 g/m^2 has the maximum drying time.

3.6. Energy analysis and drying rate

In order to analyze the energy efficiency of non-contact ultrasonic drying of hand-sheet papers, energy factor (EF) is defined as follows

$$EF = \frac{(m_i - m_t)h_{fg}}{P_{US-rad} \times t} \tag{4}$$

where m_i is the initial mass, m_t is the mass at time t, h_{fg} is the latent heat of evaporation for water at atmospheric pressure (2256 kJ/kg) and $P_{US\text{-}rad}$ is the radiated ultrasonic power to the sample. This factor is determined as the ratio of the energy required for evaporation to the ultrasonic power that is radiated to the sample. Knowing the surface area of the transducer plate (0.101 m^2) and the paper sample (0.0198 m^2), out of the total applied power to the plate (225 W), the energy radiated to the paper sample can be estimated as 44 W. This is determined by a simple view factor calculation between two parallel plates of different sizes and with negligible loss through the side openings. The view factor considers the percentage of energy leaving the transducer plate and to be incident on to the sample surface.

Table 5. Permeability measurements for non-contact ultrasonically dried paper samples.

Sample	Gurley Seconds (mean)	Std. Dev. for 5 tests	Permeability (m^2)
S-unR-150-160	12.6	0.4	5.84×10^{-14}
S-unR-200-160	12.2	0.2	6.03×10^{-14}
S-unR-150-325	42.5	1.3	3.62×10^{-14}
S-unR-200-325	40.2	3	3.83×10^{-14}
S-R-150-160	2025.1	93.7	2.27×10^{-15}
S-R-200-160	1778.31	115.5	2.58×10^{-15}
S-R-150-325	2859.2	156.8	1.78×10^{-15}
S-R-200-325	2755.1	110.2	1.92×10^{-15}

Figure 12 compares the drying rate and energy factor for different samples. The drying rate is calculated through second-order central differencing. The energy efficiency can be as high as 0.5 and the maximum drying rate is 0.58 $\frac{g}{m^2.s}$. As expected, non-contact ultrasonic drying has higher drying rate and energy efficiency at higher moisture contents. These findings agree with literature such as[18,21] for direct-contact ultrasonic drying. As the sample gets dried and moisture content decreases, the drying rate and energy efficiency decreases. A correlation is fitted to the drying curve for different samples and Table 6 summarizes the outcome. The unique advantage of these correlations is that they can be applied in physics based numerical models representing the mass flux due to ultrasound mechanism.

To confirm the effectiveness of ultrasonic drying at high moisture contents, an additional test was conducted at 800% DBMC (S-R-800-160). For this sample, the energy factor reaches to about 0.9, illustrating the impact of higher moisture content on increasing the energy factor (Figure 13). The dashed line in Figure 13 shows 100% DBMC, which is the typical moisture content at the entry of dryer section in paper drying. It is obvious that the drying rate and energy factor for moisture contents less than 100% DBMC is very low and therefore, it emphasizes the limitation of ultrasonic drying at low moisture contents. It is expected that for pure water or low consistency slurries the energy factor exceeds 1, which could have various potential applications. It should be mentioned that in the above calculations (see equation 4), the evaporation energy considered for water present in a moist paper is simply the mass times the latent heat of water. This is too idealistic as significantly more energy is needed in a conventional drying process to evaporate the water from a moist paper. This is

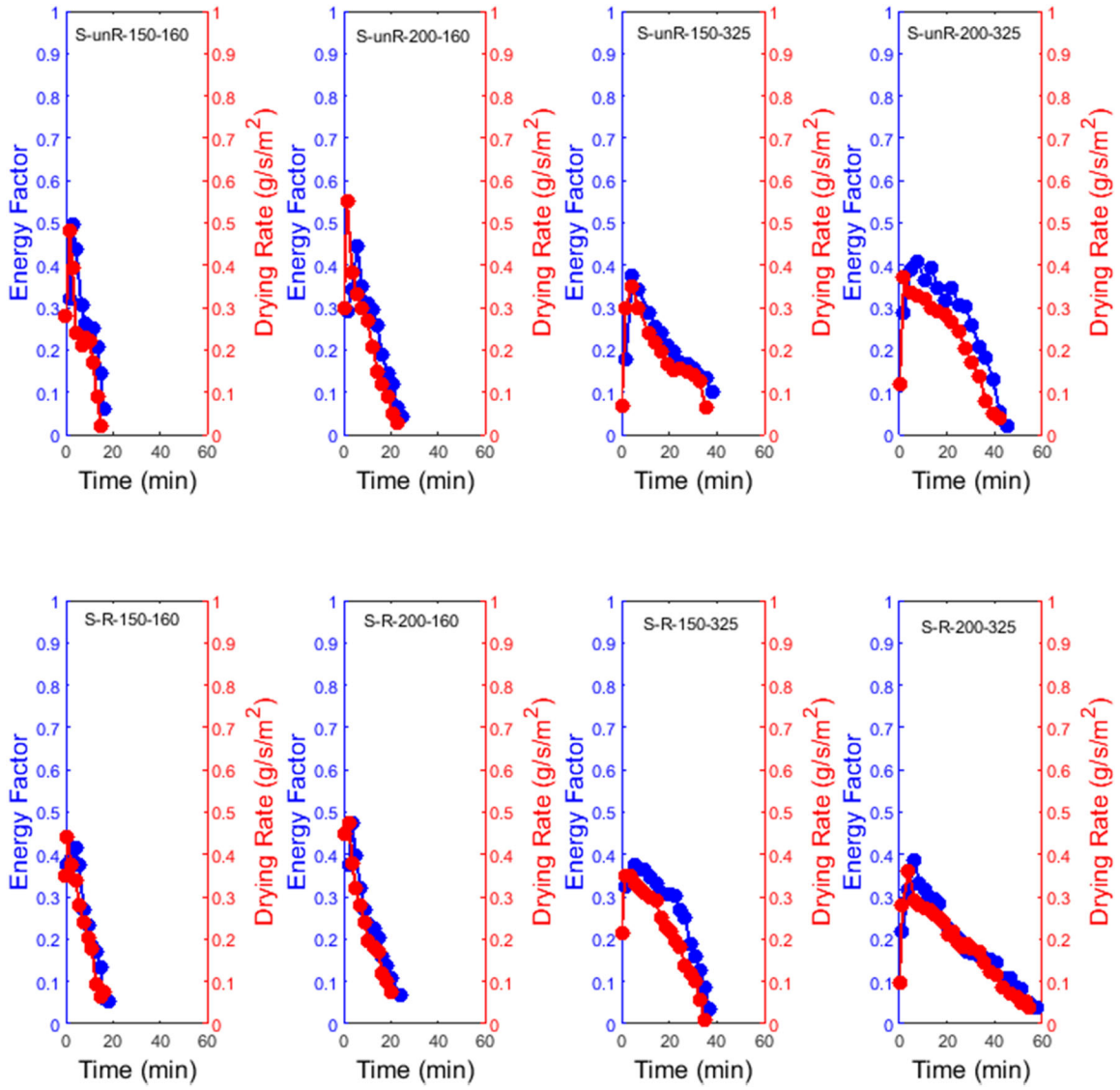

Figure 12. Energy factor and drying rate for different softwood samples. Red curve is for drying rate and blue curve is for energy factor.

Table 6. Correlation for drying rate of different samples obtained using curve fitting. For simplicity, DBMC is shown as *x*. R^2 for all the correlations is 0.99.

Sample	Correlation for Drying Rate (g/(m^2.s))
S-R-160	$10^{-7}x^3 - 3\times10^{-5}x^2 + 0.0035x + 0.0318$
S-R-325	$2\times10^{-11}x^5 - 9\times10^{-9}x^4 + 2\times10^{-6}x^3 - 0.0001x^2 + 0.0066x + 0.0007$
S-unR-160	$3\times10^{-9}x^4 - 8\times10^{-7}x^3 + 6\times10^{-5}x^2 + 0.0017x - 0.0239$
S-unR-325	$10^{-7}x^3 - 5\times10^{-5}x^2 + 0.0066x - 0.0094$

especially true at low moisture content levels (i.e., falling drying rate zone). Thus, the energy ratios for ultrasonic drying will be much higher than those presented in Figures 12 and 13. Nevertheless, the ultrasonic drying will be more effective when applied to a product with a high moisture content. In general, the energy efficiency of a typical drying process is about 50-60% and therefore, it is estimated that the energy factor for ultrasonic drying can be two times higher than the values reported in the above figures.

3.7. Comparing direct-contact and airborne ultrasonic drying

In direct-contact ultrasonic drying, the moist sample must be directly in contact with the transducer, while in airborne ultrasonic drying, the moist sample is placed underneath the transducer plate. The experiments for direct-contact ultrasonic drying are carried out at 1.7 MHz with 10 W power and airborne ultrasonic drying experiments are conducted at 21 kHz and

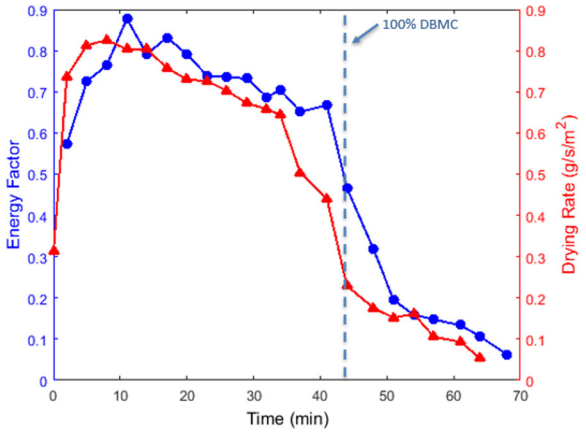

Figure 13. Illustration of the effect of high moisture content on energy factor and drying rate for S-R-800-160. The dashed line shows 100% DBMC.

225 W. The thermal heating for these two setups is compared in section 3.1 and it concluded that in direct-contact ultrasonic drying, the maximum temperature of the transducer plate is 80 °C, while in airborne ultrasonic drying, the maximum temperature is 40 °C. Therefore, the heating effect in direct-contact mechanism is substantially higher compared to that of non-contact mechanism. In the following, other aspects of drying, i.e., drying rate and energy efficiency, are compared for these two setups. The data for direct-contact ultrasonic drying is attained from Noori O'Connor et al.[18]

Since the diameter of the samples in direct-contact and non-contact ultrasonic drying is 1.98 cm and 15.9 cm, respectively, the drying rates are reported in $\frac{g}{m^2.s}$. Figure 14 compares the drying rate and energy factor for S-R-150%-160g/m^2 dried using direct-contact ultrasonic drying and airborne ultrasonic drying. The working efficiency of the two setups is assumed to be 100%.

The general trend for both mechanisms is that the drying rate is higher at higher moisture contents. However, by decreasing the moisture content, propagation of ultrasonic waves inside the sample is harder and as a result, the drying rate decreases. Therefore, the drying rate and energy efficiency for ultrasonic drying of paper at moisture contents lower than 100% DBMC, which is the typical moisture content at the entry of the dryer section, is estimated to be very low and this is a limitation for ultrasound drying of paper. The low drying rate in the beginning for direct-contact ultrasonic drying could be due to the fact that higher frequencies have lower depth of penetration inside the sample and therefore, drying has a "starting" period, initially. In addition, the drying rate for direct-contact ultrasonic drying is an order of magnitude higher than non-contact ultrasonic drying. This observation may also largely be influenced by the significant heating effect generated in direct-contact ultrasonic drying, as discussed above. Although this heating effect may not be always desirable, it has a major impact on the drying rate. Whilst the papermaking machine is in a much larger scale, it should be notified that the evaporation rate in papermaking machine is about 10 times higher than the drying rate for direct-contact ultrasonic drying according to.[25] In addition, the energy factors for direct-contact and non-contact ultrasonic drying are in the same order of magnitude. One reason for low energy factor in ultrasonic drying might be due to the bulging effect of the sample during drying, which results in imperfect contact with the transducer in direct-contact drying and increase in thickness at the edges in airborne ultrasonic drying. The energy factor could be higher and part of the loss of energy could be resolved by developing more efficient designs for the transducers. Despite the higher drying rate for direct-contact ultrasonic drying, one of the biggest challenges with this technology is that the sample must be in direct contact with the transducer and therefore it is not adaptable to the current convective dryers. In this regard, non-contact or airborne ultrasonic drying is the most ideal in terms of adapting to the convective dryers. For paper drying, one potential application of this technology is in the up-stream of papermaking machine to control moisture profile in the cross-direction and reduce overheating. For batch processes, in the cases that low temperature drying is required to preserve the properties of the products being dried, ultrasonic drying could be suitable, and it can be more efficient in hybrid with other types of drying mechanisms. Nonetheless, the outcome of this research is that at the current state, this technology is not ready for replacing the current continuous drying technologies in industrial applications, such as paper drying, and more robust and efficient designs are required. The biggest challenge in developing more efficient ultrasonic transducers is to overcome the significant impedance mismatch between air and dense mediums, which leads to substantial energy loss. There are several research groups such as[17,19,26] exploring more efficient and novel designs for ultrasonic transducers. In addition, the advantages and disadvantages of ultrasonic drying combined with other drying technologies can be explored in the future.

4. Summary and conclusions

In this study, a straightforward comparison between high-power airborne ultrasonic drying (21 kHz and

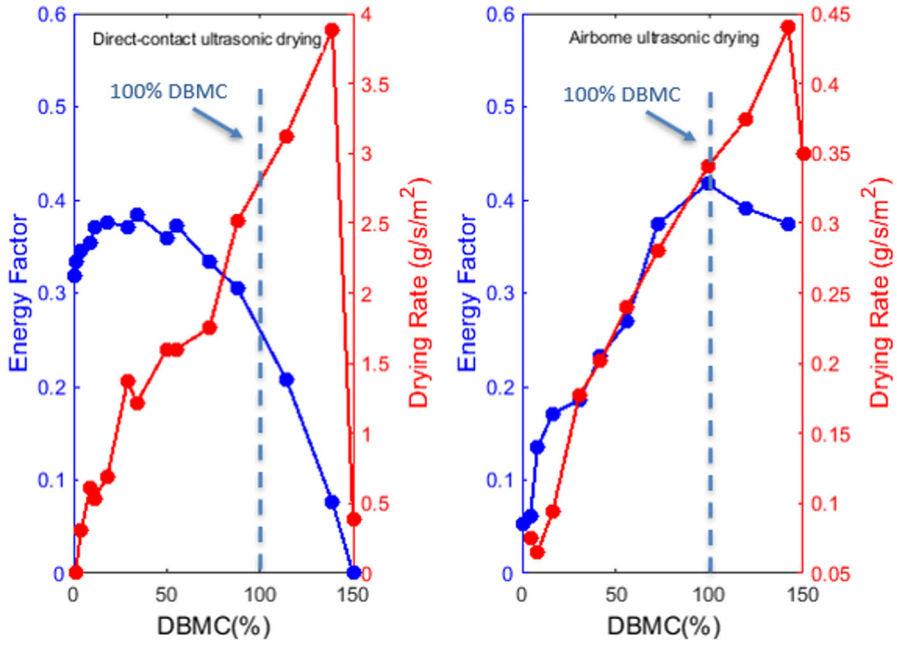

Figure 14. Comparing the drying rate and energy factor for S-R-150%-160g/m^2, dried by direct-contact (left) and non-contact (right) ultrasonic drying. Red curve is for drying rate and blue curve is for energy factor. The dashed lines show 100% DBMC.

225 W) and direct-contact ultrasonic drying (1.7 MHz and 10 W) for hand-sheet papers is provided. In conclusion, the results of 2^3 factorial design of experiments showed that for both mechanisms, basis weight/thickness of the sample has the maximum effect on total time of ultrasonic drying and after that the initial moisture content. One of the most important take-aways from this paper is that ultrasonic drying is more effective at higher moisture content and as the sample gets dried and the moisture content decreases, the drying rate and energy efficiency decrease. A correlation for predicting the total time of ultrasonic drying was obtained using linear regression analysis. Quality measurements for the dried samples by airborne ultrasonic drying agree with the measurements for samples dried with direct-contact ultrasound. Comparing to hot plate drying, the brightness index and tensile strength of the samples are slightly improved by using ultrasound mechanism. It was shown that permeability plays an important role in ultrasonic drying behavior and the effect of ultrasound for samples with higher permeability is higher. In addition, the thermal effect in direct-contact ultrasonic drying is very significant and it enhances the drying rate but may also have undesirable impact on product properties. The energy efficiency of airborne ultrasonic drying is in the same order of magnitude as direct-contact ultrasonic drying. In order to be able to use this green technology in industrial applications, more efficient designs for ultrasound transducers are required. Further details on ultrasonic drying of paper can be found in.[27]

Disclosure statement

The authors report no conflicts of interest. The authors alone are responsible for the content and writing of the paper.

Funding

This study was financially supported by the U.S. Department of Energy (DOE) Office of Advanced Manufacturing under Award Number DE-EE0009125, Massachusetts Clean Energy Center (MassCEC), and the Center for Advanced Research in Drying (CARD), a US National Science Foundation Industry/University Cooperative Research Center. CARD is located at Worcester Polytechnic Institute and University of Illinois at Urbana-Champaign (co-site). The pulps used in this study were provided by Domtar and the authors appreciate this.

References

[1] Department of Energy. Quadrennial Technology Review: An Assessment of Energy Technologies and Research Opportunities. Report by US Department of Energy. **2015**, 188–189.

[2] Sabarez, H. T.; Gallego-Juarez, A. A.; Riera, E. Ultrasonic-Assisted Convective Drying of Apple Slices. *Dry. Tech.* **2012**, *30*, 989–997. DOI: 10.1080/07373937.2012.677083.

[3] Wray, D.; Ramaswamy, H. S. Novel Concepts in Microwave Drying of Foods. *Dry. Tech.* **2015**, *33*, 769–783. DOI: 10.1080/07373937.2014.985793.

[4] Martynenko, A.; Zheng, W. Electrohydrodynamic Drying of Apple Slices: Energy and Quality Aspects. *J. Food Eng.* **2016**, *168*, 215–222. DOI: 10.1016/j.jfoodeng.2015.07.043.

[5] Yang, M.; Yagoobi, J. Enhancement of Drying Rate of Moist Porous Media with Dielectrophoresis Mechanism. *Drying Technol.* **2022**, *40*, 2952–2963. DOI: 10.1080/07373937.2021.1981922.

[6] Seyed-Yagoobi, J.; Husain, A. N. Experimental and Theoretical Study of Heating/Drying of Moist Paper Sheet with a Gas-Fired Infrared Emitter. *J. Heat Transfer* **2001**, *123*, 711–718. DOI: 10.1115/1.1372324.

[7] Loureiro, A. d C.; Souza, F. d C. d A.; Sanches, E. A.; Bezerra, J. d A.; Lamarão, C. V.; Rodrigues, S.; Fernandes, F. A. N.; Campelo, P. H. Cold Plasma Technique as a Pretreatment for Drying Fruits: Evaluation of the Excitation Frequency on Drying Process and Bioactive Compounds. *Food Res. Int.* **2021**, *147*, 110462. DOI: 10.1016/j.foodres.2021.110462.

[8] Putranto, A.; Chen, X. D. Vacuum Drying of Food Materials Modeled and Explored Using the Reaction Engineering Approach (REA) Framework. *Dry. Tech.* **2021**, *40*, 1–9.

[9] Burger, F.; Sollner, K. The Action of Ultrasonic Waves in Suspensions. *Trans. Faraday Soc.* **1936**, *32*, 1598–1603. DOI: 10.1039/TF9363201598.

[10] Gallego-Juárez, J. A.; Riera, E.; de la Fuente Blanco, S.; Rodríguez-Corral, G.; Acosta-Aparicio, V. M.; Blanco, A. Application of High-Power Ultrasound for Dehydration of Vegetables: Processes and Devices. *Dry. Tech* **2007**, *25*, 1893–1901. DOI: 10.1080/07373930701677371.

[11] Momen, A. M. **2015** Preliminary Investigation of Novel Direct Contact Ultrasonic Fabric Drying. ASME International Mechanical Engineering Congress Exposition, 57434. DOI: 10.1115/IMECE2015-50479.

[12] Fairbanks, H. V. Drying Powdered Coal with the Aid of Ultrasound. *Powder Tech* **1984**, *40*, 257–264. DOI: 10.1016/0032-5910(84)85071-8.

[13] Tao, Y.; Li, D.; Siong Chai, W.; Show, P. L.; Yang, X.; Manickam, S.; Xie, G.; Han, Y. Comparison between Airborne Ultrasound and Contact Ultrasound to Intensify Air Drying of Blackberry: Heat and Mass Transfer Simulation, Energy Consumption and Quality Evaluation. *Ultrason. Sonochem.* **2021**, *72*, 105410. DOI: 10.1016/j.ultsonch.2020.105410.

[14] Zhang, Y.; Abatzoglou, N. Fundamentals, Applications and Potentials of Ultrasound-Assisted Drying. *Chem. Eng. Res. Des* **2020**, *154*, 21–46. DOI: 10.1016/j.cherd.2019.11.025.

[15] Kowalski, S. J.; Mierzwa, D. US-Assisted Convective Drying of Biological Materials. *Dry. Tech.* **2015**, *33*, 1601–1613. DOI: 10.1080/07373937.2015.1026985.

[16] Gallego-Juarez, J. A.; et al. Power Ultrasonic Transducers with Extensive Radiators for Industrial Processing. *Ultras. Sonochem.* **2010**, *17*, 653–964.

[17] Garcia-Perez, J. V.; Ortuño, C.; Puig, A.; Carcel, J. A.; Perez-Munuera, I. Enhancement of Water Transport and Microstructural Changes by High-Intensity Ultrasound Application on Orange Peel Drying. *Food Bioprocess Technol.* **2012**, *5*, 2256–2265. DOI: 10.1007/s11947-011-0645-0.

[18] Noori O'Connor, Z.; Yagoobi, J.; Tilley, B. Experimental Study of Drying of Paper with Direct-Contact Ultrasound Mechanism. *Dry. Tech.* **2022**, 1–14. DOI: 10.1080/07373937.2022.2150635.

[19] Andrés, R. R.; Pinto, A.; Martínez, I.; Riera, E. Acoustic Field Generated by an Innovative Airborne Power Ultrasonic System with Reflectors for Coherent Radiation. *Ultras* **2019**, *99*, 105963. DOI: 10.1016/j.ultras.2019.105963.

[20] Kline, S. J. Describing Uncertainty in Single Sample Experiments. *Mech. Eng* **1953**, *75*, 3–8.

[21] Peng, C.; Ravi, S.; Patel, V. K.; Momen, A. M.; Moghaddam, S. Physics of Direct-Contact Ultrasonic Cloth Drying Process. *Energy* **2017**, *125*, 498–508. DOI: 10.1016/j.energy.2017.02.138.

[22] Colucci, D.; Fissore, D.; Rossello, C.; Carcel, J. A. On the Effect of Ultrasound-Assisted Atmospheric Freeze-Drying on the Antioxidant Properties of Eggplant. *Food Res. Int.* **2018**, *106*, 580–588. DOI: 10.1016/j.foodres.2018.01.022.

[23] Mierzwa, D.; Kowalski, S. J. Ultrasound-Assisted Osmotic Dehydration and Convective Drying of Apples: Process Kinetics and Quality Issues. *Chem. Proc. Eng* **2016**, *37*, 383–391. DOI: 10.1515/cpe-2016-0031.

[24] Mäkelä, P. Effect of Drying Conditions on the Tensile Properties of Paper. In *Proceedings of 14th Pulp and Paper Fundamental Research Symposium*, Oxford. **2009**, 1079–1094.

[25] Asensio, M. C. *Transport Phenomena During Drying of Deformable, Hygroscopic Porous Media: Fundamentals and Applications*. Texas A&M University: Michigan, USA, **2000**.

[26] Bantle, M.; Eikevik, T. M. A Study of the Energy Efficiency of Convective Drying Systems Assisted by Ultrasound in the Production of Clipfish. *J. Cleaner Prod* **2014**, *65*, 217–223. DOI: 10.1016/j.jclepro.2013.07.016.

[27] Noori O'Connor, Z. *Fundamental Understanding of Removal of Water from a Moist Porous Medium in the Absence and Absence of Ultrasound Mechanism*; Worcester Polytechnic Institute: Massachusetts, USA, **2023**.